

# Low-Power Implantable Ultrasound Imager for Online Monitoring of Tumor Growth

Abhishek Basak, *Student Member, IEEE*, Seetharam Narasimhan, *Student Member, IEEE*, and Swarup Bhunia, *Senior Member, IEEE*

**Abstract**—Clinicians all over the world agree that the most effective way to deal with a malignant tumor growth within internal organs is to detect it early. In most cases, early detection requires automated localized high resolution scanning of a region of interest – such as lungs, brain, small intestine, and gastro-intestinal tract. External or endoscopic ultrasound technologies are often not effective for imaging deep inside organs due to lack of adequate spatial resolution. In this paper, we propose using a miniature, low power implantable ultrasound imager for online monitoring of tumor growth in internal body parts. We explore the design space for such an implantable ultrasonic imaging system targeted to early detection or post-surgery monitoring of a malignant growth. The system can be placed locally in a susceptible region or for post-operative monitoring of relapse. The proposed system is capable of providing high-resolution image of a volume of interest at periodic intervals, using a relatively safe imaging technology, thus providing a chronic, reliable, and cost-effective monitoring option.

## I. INTRODUCTION

The ability to visualize lesions or abnormal masses within the body is crucial in the early detection of malignancy. Ultrasound imaging is a simple way to detect a growth and to determine whether it is a benign, fluid-filled cyst or a solid cancerous mass. Fig. 1(a) illustrates an ultrasound scan of a malignant tumor (left) and a Doppler scan (right) of such a growth, which is likely to have blood flow irregularities. Ultrasonic imaging has been used for cancer detection in breast, ovary, prostate, liver, pancreas, etc. The common practice is to non-invasively scan a region of interest by moving the transducer array on the body surface and process the received echo patterns from different depths within the body to form an image. However, external ultrasonic imaging is often incapable of producing high-resolution images throughout the entire scan volume. Higher frequency ultrasound produces high resolution images, but suffers from lower depth of penetration (greater attenuation), and hence, is unsuitable for high-resolution imaging of deeper body regions.

One recent invasive ultrasound imaging approach places the transducer assembly at the tip of an endoscopic catheter, to perform trans-esophageal, endo-bronchial, and trans-rectal imaging [1]. As the imaging is done from inside the body, the problem due to attenuation is greatly reduced. This helps in more accurate analysis of the tumor to study its characteristics and perform cancer staging. However, these

procedures can lead to great discomfort from the patient's perspective and are not suitable for chronic monitoring. Besides, there are many inner organs of interest, such as pancreas, liver, inner lung walls, and brain, which remain inaccessible to a catheter forendoscopic imaging. Hence, there is need for a system capable of performing automated online high-resolution imaging of inner body structures, both for early detection of anomalous growth as well as for monitoring post-treatment recurrence.

In this paper, we propose the concept of an implantable ultrasound imaging system, which can be surgically implanted to provide high-resolution images for a volume of interest. Ultrasound is a relatively safe imaging technique involving no ionizing radiation and strong magnetic fields. Fig. 1(b) and (c) illustrate the advantages of the proposed system over external and endoscopic techniques. We study the feasibility of such a system by identifying important design parameters and investigating placement considerations of the implants and their power requirement.

For early detection of malignancy, the imager can be implanted in a person with high risk of cancer during surgery (for a different purpose). People with ulcerative colitis or Crohns disease are susceptible to colon-rectal cancer [2]. An ultrasound imager may be implanted during surgical removal of appendix to monitor the intestinal walls for early detection of potential malignancy development. Statistical trends show that people with high alcohol intake, who have a history of diabetic or obesity problems, or have been diagnosed with gallstones, have high chances of contracting liver, pancreatic or gall bladder cancer [2]. During a gallstone removal surgery, an imager can be implanted to monitor the adjoining regions for periodic (e.g. monthly) screening. In case of patients who undergo surgical removal of malignant lesion, the imaging assembly can be implanted in the region of malignancy. Frequent high-resolution images of the malignant region are required to monitor the progress of treatments of cancer patients, e.g. proper dosage of chemotherapy, effectiveness of the drugs, and potential spread of cancer. An imaging assembly, deployed within the volume of interest is capable of providing images of the highest resolution.

The major contributions of the paper are as follows. 1) It proposes a novel implantable imaging assembly for early detection and post-treatment monitoring of cancerous growth. It can enable reliable online monitoring of a region of interest deep within the body. 2) It describes the design considerations and explores the parameter space for such a system. 3) It presents a case study for deployment of the proposed system and studies the power requirement.

The authors belong to the Electrical Engineering and Computer Science Department, Case Western Reserve University, Cleveland, OH, USA-44106. Email: {axb594, sxn124, skb21}@case.edu.

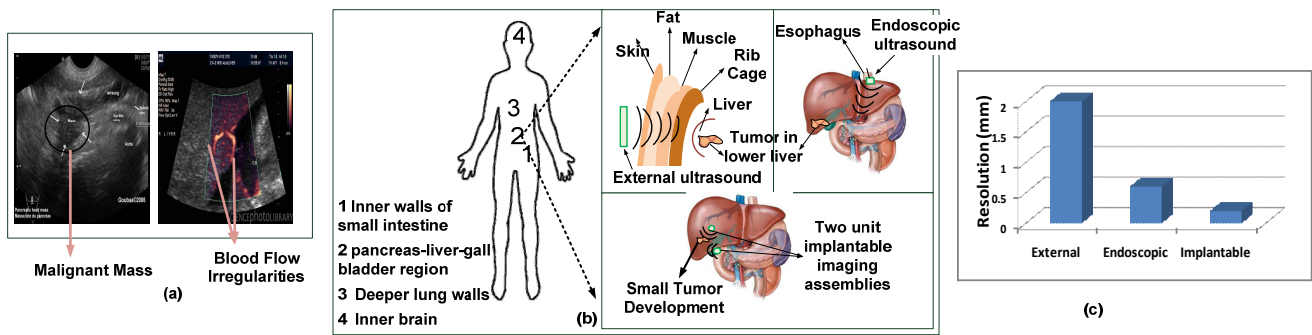


**Fig. 1: (a) Pancreatic carcinoma ultrasound (left) and increased blood flow (shown in orange) in the cancerous region in Doppler image (right). (b) Advantages of implantable imager for high resolution local monitoring compared to external and endoscopic ultrasound. (c) Comparison of resolution between proposed implantable imager and external and endoscopic ultrasound.**

## II. OVERALL SYSTEM ARCHITECTURE

Our imager constitutes of transducer assemblies, placed at different points within a region of interest for scanning the entire volume with a uniform spatial resolution ( $\sim 0.1$  mm). Images from each assembly are stitched together to obtain the tomographic 3-D rendered image of the entire region of interest. A system diagram of the proposed setup is shown in Fig. 2(a). Each imaging assembly consists of two main parts: 1) **Hardware** – The main hardware components include the transducer assembly, the front end electronics, micro-motors (for rotation of transducers for entire scan coverage) and transceivers for wirelessly sending compressed images. 2) **Software**– The software part consists of algorithms for image reconstruction and stitching, feature extraction for detection of anomalies/irregularities and image compression for transmission to an external computer for further analysis.

## III. DESIGN CONSIDERATIONS

Design of the hardware system involves calculating the parameters for a unit transducer array, spatially arranging the arrays in a unit assembly and finally placing the transducer assemblies for best volume coverage. The design methodology is developed as a bottom-up approach (Fig. 2 (b)), with three main stages as described below:

1) **Design of the basic transducer array:** In this stage, the transducer frequency, array type, aperture length, pitch of elements, etc. are determined. The depth of imaging of the transducer array is calculated, which sets the radius of a unit spherical volume that can be scanned by a single transducer assembly. For detecting cellular-level anomalies the required

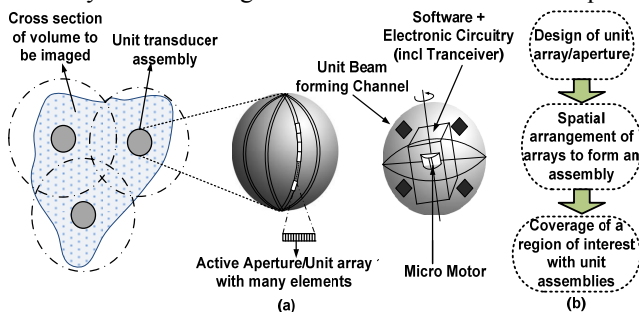


**Fig. 2: (a) The implantable ultrasonic imaging system consists of one or more implants with surface-embedded transducer arrays. Micro-motors and electronics are encapsulated in a spherical assembly. (b) Bottom-up approach for system design.**

axial, lateral and slice thickness resolution is  $\sim 0.1$  mm.

**Axial Resolution** - The axial resolution determines the ultrasound pulse frequency. The wave pressure at a depth  $x$  from the transducer along the direction of propagation can be approximated as  $P = P_0 e^{-\alpha(f)x}$  where  $P_0$  is the transmitting wave pressure at the transducer surface. In our design,  $\alpha(f) = \alpha_1 \cdot f$ , with a linear frequency dependence and attenuation coefficient  $\alpha_1 = 0.5$  dB/cm/MHz. The dynamic range of our system is assumed to be 100 dB. Considering the round trip echo path, the variation of depth of imaging with frequency is illustrated in Fig. 3(a). The depth corresponding to our desired frequency of 31 MHz is 3.23 cm. The peak spectral frequency reduces with increasing depth of propagation. Axial resolution would start to degrade if the peak central frequency gets reduced by more than 1 MHz, which happens around 50 cm ( $\gg 3.2$  cm) [3]. So, according to calculations shown in Fig. 3 (b), the ultrasound frequency = 31 MHz.

**Lateral Resolution** - Our basic unit is a phased transducer array consisting of rectangular elements. Phased arrays provide the advantage of electronic beam steering and focusing, with the best resolution achieved at the focal point. The design parameters are the number of elements in an active aperture, pitch of the elements, height of the elements, etc. By the use of a phased array, we implement dynamic focusing in the azimuthal plane, to obtain uniform resolution at different depths. We select the -6 dB beam-width or the full width half maximum (FWHM) as the basis for calculating the lateral resolution at different ranges. At a distance  $F$ , for an active aperture of length  $L$ ,  $FWHM = 1.203 \cdot \lambda \cdot F/L$ , where  $\lambda$  is the pulse wavelength. The beam can be dynamically focused only up to the transition zone (from near to far field), calculated as  $L^2/\lambda$ .

For a particular ultrasound frequency, larger the active aperture length, better is the beam directivity. On the contrary, for a particular element size (usually around 50-100  $\mu$ m), the larger the aperture, the larger the number of elements required per aperture, resulting in increased complexity in construction, front-end electronics as well as higher power requirement. Besides, each of these phased array units will be embedded on the surface of a unit sphere (enclosing the front-end electronics, and interconnects) of radius  $\sim 1.2$  cm. An array unit/aperture placed along the circumference ( $C = 2 \cdot \pi \cdot 1.2 = 7.54$  cm) of the central circle should be  $\sim 4$  mm, the length ratio being 5% (approximately linear). In order to achieve a uniform lateral resolution of 0.1

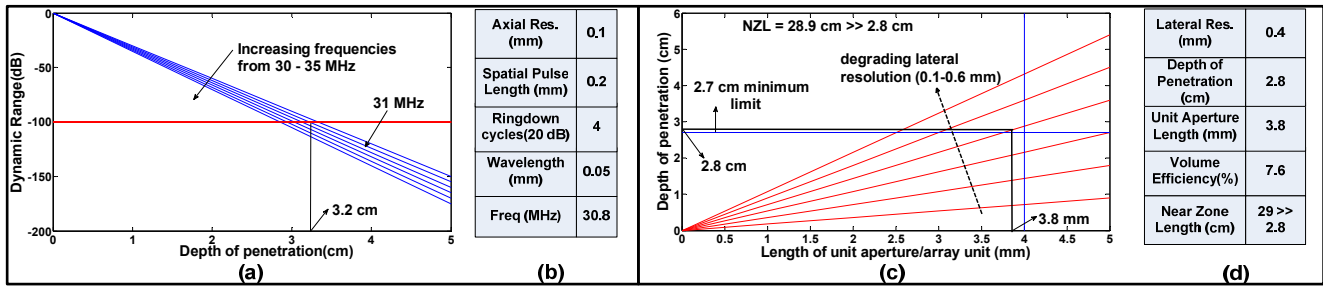


**Fig. 3: (a) Variation of depth of penetration with ultrasound frequency and with allowable dynamic range. (b) Table showing calculation of transducer frequency. (c) Variation of length of unit aperture/ array unit with depth of penetration for different values of lateral resolution. (d) Table showing maximum range/depth of penetration calculation.**

mm,  $F/L = 1.7$ . For an aperture length of 4 mm, the focal length is  $\sim 7$  mm  $\ll 3.23$  cm. To increase the depth of focus, we need to compromise on the lateral resolution as shown in Fig. 3 (c). The maximum range, to obtain the desired spatial resolution, should not be less than 2.7 cm, as the volume ratio, considering a unit assembly of radius 1.2 cm, is  $\sim 8\%$ . A compromise is achieved from the plot, with the parameters shown in Fig. 3 (d). The radius of the spherical volume, scanned with uniform spatial resolution, is 2.8 cm.

Dynamic focusing both on transmit and receive side would improve the sensitivity and accuracy of detection. Having multiple focal zones on the transmit side helps to achieve uniform lateral resolution. For an active aperture,  $\sim 10$  dynamic focusing zones (zone from 1.5 times the minimum beam width to the focus) are required for covering the range of 2.8 cm. It also leads to temporal averaging and hence, speckle reduction by  $\sim 3.2$  times ( $\sqrt{10}$  times ([5])).

**Slice Thickness Resolution** - For slice thickness resolution, dynamic focusing in the elevation plane is achieved through the use of 2-D arrays. However numerous complexities arise with 2-D arrays [4] which limit the highest achievable pulse frequency to 10 MHz. Alternately, acoustic lens, composed of epoxy material, can be used to achieve a fixed focus in the elevation plane. Hence, 3 consecutive array units are covered with acoustic lens of focal lengths 0.5, 1.5, and 2.5 cm and a resolution of 0.1 mm at the focus. The height of the elements is 0.5 mm and rotation is used to achieve focusing.

To avoid spurious reflections, grating lobes need to be minimized. If the pitch of the elements is  $\lambda/2 \sim 26 \mu\text{m}$  (the spatial Nyquist rate), the number of elements required per aperture is  $\sim 150$  (= no. of Tx/Rx channels in each beam-forming unit). Fig. 4(a) illustrates the variation of number of elements/aperture and maximum beam steering angle with element pitch. Accordingly, a pitch of  $38.5 \mu\text{m}$  is selected, with a maximum beam steering of around  $25^\circ$ , considering 98Tx/Rx channels per aperture due to power constraints.

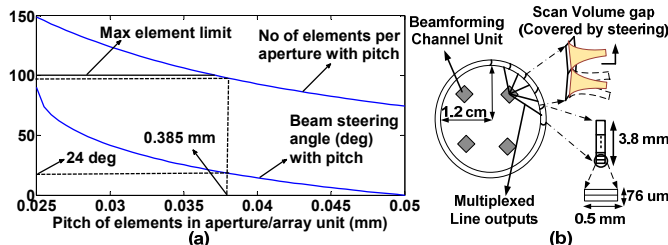


**Fig. 4: (a) Variation of no. of elements/aperture and beam steering angle with element pitch. (b) Array units forming unit assembly.**

**2) Spatial arrangement of transducer arrays to form a unit assembly:** The array units (of length 3.8 mm with 98 elements of pitch =  $38.5 \mu\text{m}$ ) will be sequentially attached along the circumference of longitudinal circles on the surface of the spherical assembly as a curvilinear phased array of radius 1.2 cm, as illustrated in Fig. 2(a). Longitudinal circles passing through the two vertex points of the sphere are of same length. Considering a unit circle of the spherical assembly of radius 1.2 cm, the number of apertures/array units = 20. We consider 4 beam-forming units, each with 98Tx/Rx channels controlling a quarter of the circle with 5 apertures (Fig. 4(b)). In order to cover the scan gap between two consecutive apertures, we use steering of the transmit beam, which also provides accurate information regarding orientation and size of anomalous objects from the direction and intensity of reflected echoes. As the maximum beam steering angle in our assembly is  $\sim 25^\circ$ , we steer the transmit beam along  $12^\circ$  and  $25^\circ$  in either direction. This would correspond to 5 transmit zones with 10 multiple focuses per zone for an aperture.

Due to construction complexities and requirement of a large number of active beam forming channels, we do not cover the entire sphere surface with circles. We use 16 longitudinal circles and perform rotation (30 rotations with 60% overlap) in the axial plane to cover the volume gaps.

**3) Spatial positioning of transducer assemblies for best coverage of a region of interest:** In the case of during (or post) treatment monitoring, the affected region is known and its maximum volume is generally  $\sim 10\text{-}20 \text{ cm}^3$ , provided it has not reached the metastatic stage. One transducer assembly covering a depth of 2.8 cm (sphere of volume of  $\sim 90 \text{ cm}^3$ ) is enough for monitoring the malignant region. However, for early detection of cancer, where the region is

**Table 3: Unit Aperture Design Parameters**

Resolution (mm)	Range		Unit Aperture Operation					
	Depth (cm)	Vol %	Pitch ( $\mu\text{m}$ )	No of elements	Height (mm)	Focus zones	Steering (deg)	
Axial	0.1	2.8	7.6	38.5	98	0.5	10	(12 *2)
Lateral	0.4							
Elevation	0.1							

**Table 4: Unit Assembly Design Parameters**

Rotation (deg)	Unit transducer assembly (radius = 1.2 cm) (scan range = 2.8 cm)					
	No of curvilinear arrays	No of apertures/ circle	No of Tx/Rx units	Peak Power (mW)	Scan Freq (Hz)	Energy (J)
Axial (0.07 * 30)	16	20	(4*2 = 8)	240	50	288
Long. (3*2)						

not known beforehand, we choose a larger volume of interest depending on its susceptibility to contract cancer, cancer statistics, etc. We consider the pancreatic region to visualize the placing of unit assemblies.

#### IV. RESULTS

The calculated design parameters for construction of a unit array/aperture and a unit imaging assembly are shown in Table 3 and Table 4, respectively. Next, the estimated power requirement for a unit transducer assembly is provided.

**Power Requirement:** The power requirement (considering Tx/Rx switches, amplifier, pulser, etc) of a (16×16) element, 5MHz transducer is ~8.5mW. In our application, an aperture contains 100 elements at 30MHz frequency. Considering a linear dependence, the power requirement per Tx/Rx action of our assembly per aperture would be around ~30mW. The peak power, a critical parameter for implantable system design, depends on the number of active apertures per circle and the number of active circles at a particular time instant. In our system, considering 4 apertures per circle (one per quarter) and 2 longitudinal circles (which intersect perpendicularly at the vertices), the peak power for 8 Tx/Rx beam forming units would be 240mW. The upper limit for the time between 2 scan operations is the go-return time required by a pulse to cover a depth of 2.8 cm (0.02 ms). The resulting frequency is 50KHz. We operate at a much lower frequency of 50 cycles/sec, the duty factor of the pulses being  $6.5 \times 10^{-5}$ , for low power operation. A typical MEMS motor requires around 310nW input power at an efficiency of 42% and 300 rev/min [6]. By using ultralow-power ASIC for scan operations, where for a scan frequency of 50Hz and pulse frequency of 30MHz, the power per Tx/Rx is ~1.8mW [7], the estimated peak power and energy requirement would be only ~15mW and 18J respectively. According to the American FDA, the spatial peak temporal intensity  $I_{SPTA}$  needs to be within  $720 \text{ mW/cm}^2$  to prevent excess tissue heating during imaging [3] and the spatial peak pulse average intensity ( $I_{SPPA}$ ) responsible for mechanical cavitation effects in tissues is limited to  $150 \text{ W/cm}^2$ . Our system satisfies this, as shown in Fig. 5.

**Case Study:** Translating the endoscope to the pancreatic region through the esophagus is difficult as the pancreas is located behind the stomach plane. Pancreatic cancer is a major disease with high mortality rates [2]. Presently when tumors are detected in pancreas, it has 40-50 % chance of being cancerous. Besides regions around the pancreatic head like bile duct, gall bladder, lower liver are also susceptible to cancer [2]. Monitoring the region (shown approximately in Fig. 6(a)) through the implantable imager would be beneficial. The monitoring region is approximately a sphere of radius 4 cm (pancreatic head with radius ~2.3 cm, rest includes duodenum walls, lower liver, bile duct, and a part

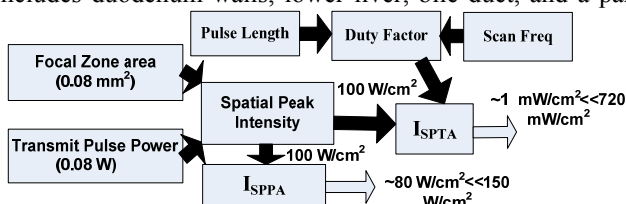


Fig. 5: Imaging system satisfying  $I_{SPTA}$  and  $I_{SPPA}$  constraints.

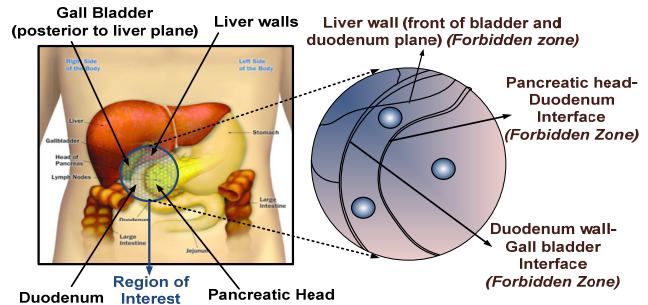


Fig. 6: (a) Region of interest in our case study. (b) Placement of 3 assemblies for scan coverage considering forbidden zones.

of gall bladder). This sphere of radius 4 cm is decomposed into unit scan volumes (sphere of radius 2.8 cm). However a unit assembly cannot be placed anywhere due to different anatomical features, difficulty in surgically placing it, mechanical stability considerations after implant, etc. For instance, the interface between the pancreatic head and duodenum wall, intersection region of lower liver and duodenum are not suitable for placement of assemblies. In 2-D, the problem reduces approximately to filling the area of a circle of radius 4 cm with unit circles of radius 2.8 cm, with certain forbidden regions. While covering the entire region of interest, there might be trade-offs between region of overlap and extension of scan area beyond the intended volume. Our obtained solution (as shown in Fig. 6(b)) is to fill the sphere ( $r = 4 \text{ cm}$ ) with 3 unit imaging spheres.

#### V. CONCLUSION

We have presented the concept of an implantable ultrasonic imaging assembly for online monitoring of tumor growth – both new and recurrence – in internal body parts at near-cellular level resolution. The primary advantages of such a system over existing techniques – external or endoscopic – are the high spatial resolution over a volume of interest at deep internal regions of the body and online monitoring, facilitating point-of-care applications. We have presented detailed study on the hardware design space to meet constraints on operating power, size, placement and spatial resolution of the recorded image. Such an assembly could also be used for ultrasound-guided biopsy or for treatment of a growth. Future work would include developing the software components and validating a prototype system with animal experiments.

#### REFERENCES

- [1] O. Cladeet *et al*, "10 MHz Ultrasound linear array catheter for endo bronchial imaging," *IEEE International Ultrasonics, Ferroelectrics and Frequency Control 50<sup>th</sup> Anniversary Conference*, 2004.
- [2] <http://www.cancer.gov/cancertopics>.
- [3] T. L. Szabo, "Diagnostic Ultrasound Imaging Inside Out," *Elsevier Academic Press*.
- [4] S. W. Smith *et al*, "Two dimensional arrays for 3-D ultrasound," *Proceedings of Ultrasonics Symposium*, 1545-1553, vol. 2, 2002.
- [5] G. E. Trahey *et al*, "Speckle pattern correlation with lateral aperture translation: Experimental results and implications for spatial compounding," *IEEE Trans. UFFC*, pp. 257-26, 1986.
- [6] S. Merzaghi *et al*, "Development of a hybrid MEMS BLDC Micromotor," *IEEE Transactions on Industry Applications*, 2011.
- [7] J. Johansson *et al*, "Ultra-Low power transmit/receive ASIC for battery operated ultrasound measurement systems," *Sensors and Actuators A: Physical*, vol. 125, Issue 2, Jan 2006.